



Published in final edited form as:

Biochemistry. 2009 June 9; 48(22): 4838–4845. doi:10.1021/bi900166y.

Crystal Structure Of The Human Lymphoid Tyrosine Phosphatase Catalytic Domain: Insights Into Redox Regulation^{†,||}

Sophia J. Tsai^{‡,⊥}, Udayaditya Sen^{‡,⊥}, Lei Zhao[§], William B. Greenleaf[‡], Jhimli Dasgupta[‡], Edoardo Fiorillo[§], Valeria Orrù[§], Nunzio Bottini^{§,*}, and Xiaojiang S. Chen^{‡,*}

[‡] Molecular And Computational Biology, University of Southern California, Los Angeles, CA 90089

[§] Department of Biochemistry and Molecular Biology, The Institute for Genetic Medicine, University of Southern California, Los Angeles, CA 90033

Abstract

The lymphoid tyrosine phosphatase LYP, encoded by the PTPN22 gene, recently emerged as an important risk factor and drug target for human autoimmunity. Here we solved the structure of the catalytic domain of LYP, which revealed noticeable differences with previously published structures. The active center with a semi-closed conformation binds phosphate ion, which may represent an intermediate conformation after de-phosphorylation of the substrate but before release of the phosphate product. The structure also revealed an unusual disulfide bond formed between the catalytic Cys and one of the two Cys residues nearby, which is not observed in previously determined structures. Our structural and mutagenesis data suggest that the disulfide bond may play a role in protecting the enzyme from irreversible oxidation. Surprisingly, we found that the two non-catalytic Cys around the active center exert an opposite yin-yang regulation on the catalytic Cys activity. These detailed structure and functional characterizations have provided new insight into auto-regulatory mechanisms of LYP function.

Regulating tyrosine phosphorylation level is a fundamental mechanism for numerous important aspects of eukaryote physiology, as well as human health and disease (1-3). Cellular tyrosine phosphorylation levels are regulated by the antagonistic activities of two classes of enzymes, the protein tyrosine kinases (PTKs)¹ and the protein tyrosine phosphatases (PTPs). Recent findings have led to the emerging recognition that PTPs play specific and even dominant roles in setting the levels of tyrosine phosphorylation in cells and in the regulation of many physiological processes (2-7). Disruption of the equilibrium maintained by PTPs and PTKs causes a range of human disease, including cancer, diabetes, and autoimmunity (8-16).

A major class of PTPs, known as classical PTPs, include transmembrane PTPs and non-receptor PTPs (NRPTP), which are then further sub-classified based on their sequence similarities and non-catalytic domain structural motifs (4,8). NRPTPs display various

^{||}The coordinates and structure factors for the disulfide structure of PTPN22 (PDB ID: 3H2X) have been deposited in the Protein Data Bank.

[†]This work is supported in part by National Institutes of Health (AI055926 Grant to X.S.C.) and a Juvenile Diabetes Research Foundation International (AI070544 Grant to N.B.)

*To whom correspondence should be addressed: nunzio@usc.edu, Institute for Genetic Medicine, University of Southern California, Los Angeles, CA 90033; or xiaojiang.chen@usc.edu, Molecular And Computational Biology, University of Southern California, Los Angeles, CA 90089. Tel.: 213-740-5487; Fax: 213-740-4390.

[⊥]These authors contributed equally

¹Abbreviations used in the text: protein tyrosine kinases, PTKs; protein tyrosine phosphatases, PTPs; non-receptor PTPs, NRPTP; lymphoid-specific tyrosine phosphatase, LYP; cysteine, Cys; reactive oxygen species, ROS; catalytic domain of LYP, LYPCat; catalytic cysteine, catC227; 6,8-difluoro-4-methyl umbelliferyl phosphate, DiFMUP

intracellular localizations, determined by amino acid sequences outside the catalytic domain. The lymphoid-specific tyrosine phosphatase (LYP) encoded by the PTPN22 gene is a classical NRPTP (belonging to the NT4 sub-family), expressed exclusively in cells of haematopoietic origin. LYP, an intracellular 105 kDa protein that contains two distinct functional domains, acts as an inhibitor to down regulate T-cell activation (17) by dephosphorylating lymphocyte receptor tyrosine kinases (SRC family). The N-terminal portion of LYP contains a single tyrosine phosphatase catalytic domain and the non-catalytic C-terminal region contains four proline rich SH3 domains.

The importance of LYP in immune system regulation has been recently demonstrated by the finding that a human variant W620, caused by a single nucleotide polymorphism in PTPN22 at nucleotide 1858, leads to a significantly increased risk for autoimmune diseases including type-1 diabetes, rheumatoid arthritis and systemic lupus erythematosus (11,16,18,19). Since the autoimmune-predisposing LYP-W620 variant is a gain-of-function mutation and shows increased phosphatase activity (20), LYP is currently considered a promising drug target for autoimmunity. Elucidation of the structure and regulation of LYP is important in order to understand its mechanism of action in autoimmunity and to develop innovative approaches to the pharmacological inhibition of the enzyme for therapeutic purposes.

One possible mechanism of regulating cysteine-based PTP activity is through oxidation of the catalytic cysteine (Cys). PTPs are differentially oxidized and inactivated *in vitro* and in living cells. Many stimuli, including growth factors, cytokines and ultraviolet light induce the production of reactive oxygen species (ROS) capable of shifting the cellular redox state towards oxidation. Oxidation of the active site Cys, a soft target because of its low pKa, abrogates its nucleophilic properties and inactivates the enzyme. There has been accumulating evidence that at least part of the cellular responses to these stimuli are due to the specific and transient inactivation of the PTPs (21,22), indicating that PTPs are important sensors of the cellular redox state and that oxidation of PTPs is emerging as an important regulatory mechanism.

Thus far, three mechanisms have described the redox regulation in the PTP superfamily. One mechanism involves a disulfide bridge formation between the catalytic Cys and a second Cys found within the signature motif followed by reactivation through reduction of the catalytic Cys. This method of protecting the active-site Cys has been shown in the low molecular weight protein tyrosine phosphatase (23-25). Another similar mechanism involving disulfide formation is seen in PTEN and Cdc25 (12,26-29). Third, the redox mechanism seen in classical PTPs involves the formation of a reversible sulfenamide ring by the catalytic Cys with the main-chain amide of the next residue, namely serine, within the signature motif and thereby protecting the catalytic Cys from damage by ROS. This type of mechanism has been previously described in PTP-1B (30,31).

In this paper, we describe the crystal structure of the catalytic domain of LYP (named here as LYPcat) that has a bound phosphate ion at the active site and has a closed conformation for the active site loop. The active site of LYP consists of a catalytic Cys residue that is within bonding distance of two additional Cys around the active center in the 3-D structure, which is unique to LYP subfamily. The structure reveals a disulfide bond not previously seen in classical PTPs between the catalytic Cys (catC227) and the Cys residue (C129) outside the signature motif (or back-door Cys) that is conserved only in LYP and its close homologs, PTP-PEST and BDP1. We also found that a secondary P-loop Cys (C231) may function as a negative regulator of LYP activity. Our structural and mutational data suggest that in LYPcat, the two non-catalytic Cys around the active center may play an important yin-yang regulatory role on the enzyme activity, possibly through redox reactions to influence the catalytic Cys.

Experimental Procedures

Reagents

Hydrogen peroxide (H₂O₂, VWR) was fresh diluted from the stock solution. PTP activity was assayed using 6,8-difluoro-4-methyl umbelliferyl phosphate (DiFMUP, Invitrogen) as the substrate.

Cloning, Expression, and Purification

LYPcat (residues 2-309) was cloned into the pET28a expression vector and sequenced. The transformed vector was expressed in *Escherichia coli* BL21(DE3) cells. Expression was induced with 0.2 mM isopropyl-1-thio- β -D-galactopyranoside, and the cells were grown overnight at 25°C. Cells were harvested by centrifugation and re-suspended in 50 mM Tris-HCl, pH 8.0, 300 mM NaCl, and 5 mM β -mercaptoethanol. Cells were lysed by a microfluidizer and then centrifuged at 13,000g. The His-tagged protein was purified using a Ni²⁺ affinity column (Qiagen) following standard protocols. The resin was incubated overnight with 50 units of thrombin to remove the His-tag. Eluted protein was further purified by gel filtration using a Superdex-75 column (GE Lifesciences). The purity and integrity of the protein was checked by SDS-PAGE. The eluted protein was concentrated to 18mg/ml for crystallization experiments.

Mutants were prepared using the Quikchange protocol (Stratagene) and confirmed by DNA sequencing. Procedures for purification of all mutants are the same to that described for wild-type LYP.

Crystallization and Data Collection

Crystals of LYPcat were obtained using hanging drop vapor diffusion method at 18°C using a precipitant containing 2.0 M ammonium sulfate, 0.2M sodium-potassium phosphate in 0.1M MES, pH 6.2. Plate shaped crystals were flash frozen after a quick soaking in a cryo solution containing 10% glycerol, 2.0 M ammonium sulfate, 0.2M sodium-potassium phosphate in 0.1M MES, pH 6.2 and diffraction data up to 2.2Å were collected at an in-house R-AXIS IV+ image plate (Rigaku). The data was processed using HKL2000, and data statistics are shown in Table 1.

Structure Determination and Refinement

The structure of LYPcat was initially solved by molecular replacement method (AMoRe, CCP4 suite)(32), using the crystal structure of human protein tyrosine phosphatase receptor type J (PTPRJ; PDB ID: 2CFV) as a search model with the closest sequence similarity to LYP available in the data bank at the time. Since PTPRJ has a low sequence identity (39%) with LYPcat, a poly-alanine model was used to succeed in finding the solution. The solution was refined by rigid body and positional refinement and the electron density map was calculated with CNS and displayed on Silicon Graphics workstations using 'O'. The previously removed helices, loops and the side chains were gradually added to the model, guided by the electron density map, and the model was refined using the standard slow-cool and positional refinement protocols of the CNS package using the data between 20 to 2.2 Å. The free R value was calculated throughout by randomly selecting 5% of the data as the test set. Inclusions of side chains, water molecules, and the bound phosphate ion coupled with a few cycles of refinement yielded good refinement statistics (Table 1).

PTP activity assay

The PTP activity of the purified LYPcat was assayed in a 96-well plate in a total volume of 100 μ L, containing 0.05M Tris-HCl pH 7.4, 0.05 μ M of wild-type and the C129S mutant,

0.15 μ M of the C231S and C129S-C231S mutants, and 0.1 mM DiFMUP. In order to compare each assay to a fully active enzyme, controls were reactivated with 10 mM dithiothreitol (DTT) for 15 minutes before the assay. Inactivation was achieved by oxidation through incubation with 1.0 mM H₂O₂ for 10 minutes. Reactivation of oxidized wild-type and mutants was achieved by incubation of the inactivated enzymes with 10 mM DTT for 15 minutes. All incubations were performed at 25°C and data recording at 37°C in a Wallac Victor Microplate Reader (PerkinElmer). DiFMUP fluorescence signal was measured at an excitation of 355nm and an emission of 460nm in the microplate reader at approximately one time per minute for 8 minutes to assess linearity of the reaction.

Calculations of specific activity and % reactivation

Calculation of specific activity were done by creating a standard curve of varying concentrations of DiFMU, to get the rate of product formation. This rate is then divided by protein concentration and time to get specific activity. To get the % of reactivation using DTT after inactivation of the enzyme by H₂O₂, the reactivated activity of each mutant was divided by its full activity before inactivation.

Statistics

To check for statistic significance, p-values for the paired t-test were calculated using the GraphPad QuickCalcs Web site: <http://www.graphpad.com/quickcalcs/ttest1.cfm> (accessed September 2008).

Results & Discussion

Crystal structure determination

LYPcat (residues 2-309 of LYP) crystallizes in the spacegroup P21 with one molecule in the asymmetric unit. The three dimensional structure of LYPcat has been refined to a crystallographic R-factor of 17.6% (Rfree 20.4%) and the accuracy of the refined model is consistent with the quality of the diffraction data (Table 1). The 2Fo - Fc map for the entire polypeptide chain is well defined except for the N-terminus His-tag and a few C-terminus residues (303-309). Unambiguous electron densities are observed for all surface loops (Fig. 1A), including the PTP signature motif that forms the catalytic pocket (P-loop, residues 226-233), the pTyr recognition loop (confers specificity to pTyr, residues 54-60), the WPD loop (contains the general acid-base catalyst D195, residues 193-204), and the Q-loop (contains the conserved Q274 required to position and activate a water molecule for nucleophilic attack, residues 274-301) (Fig. 1A, 2B).

Overall, our structure is similar to the previously published LYP structures (33,34), however, noticeable differences in some important loops are noticed. While the pTyr recognition loop, Q-loop and P-loop appear unchanged, the WPD loop around the active center shows an $\sim 8\text{\AA}$ difference between the open and closed states in the various structures. In our structure, the WPD loop appears to be in an intermediary stage between open and closed forms (Fig. 1B-1D, see also below). In addition to the changes noted in the major surface loops, we can see differences in the LYP-specific loop at the end of helix $\alpha 2'$, which, as noted previously, takes on different conformations depending on the binding state of the protein (33). Moreover, a disulfide bond between catC227 and C129 is observed in our structure, which is not present in the previously reported structures (33).

Catalytic pocket of LYPcat

The phosphotyrosine binding site is a deep pocket on the surface of LYPcat. Electrostatic potential calculation shows that the bottom of the phosphotyrosine binding pocket has a strong

positive charge (Fig. 2A). Interestingly, a clear electron density corresponding to a phosphate ion is observed in this active site cleft of our structure (Fig. 2A). The detailed interactions between the bound phosphate, which could mimic the substrate/product of PTP, and the P-loop (Fig. 3) are discussed below. While primary sequence alignments and structures of other PTP superfamily members have just one Cys residue close to the catalytic Cys, our LYPcat structure reveals two Cys residues, C129 and C231 in the vicinity of the catalytic C227 (catC227). Sequence alignments with other classical PTPs reveal that these Cys are highly conserved in LYP and its close homologs PTP-PEST and BDP1, all of which belong to NT4 sub-family (Fig. 2B). The residue corresponding to C129 is strictly threonine or asparagine in other classical human PTPs and the residue corresponding to C231 is mostly threonine or valine (9). In our structure, a disulfide bond is formed between catC227 and C129, which is in a reduced state in previously reported structures (33). This disulfide bond formation is not feasible in other classical PTPs due to the lack of the equivalent Cys residue. C129 in our structure is spatially close enough to catC227 to make the disulfide bond, although it is relatively distant by primary sequence (Fig. 2B, 2C). This arrangement is known in other PTP classes as a back-door Cys (12,29).

Movement of the WPD loop

WPD loop movement has been shown to be important in PTP substrate binding. The WPD loop of the structure in this report is in a half-closed state (Fig. 1C, 1D). The disulfide bond observed between catC227-C129 restricts movement of the β 3- β 4 loop, preventing full closure of the WPD loop over the active site. In addition, the strong stacking interaction between W193 of the WPD loop and the guanidinium group of R233 in the P loop observed in our structure (Fig. 3A) must be broken, as seen in closed-form structures in the LYP-apo and tungstate-bound PTP-1B (PDB IDs: 2P6X and 2NHQ), before the WPD loop can move close enough for phosphatase activity to begin. Interaction of W193 and the invariant R233 found in the P-loop plays an important role in the closure of the WPD loop (9). In our structure of LYPcat, R233 adopts an extended conformation and is engaged in a strong stacking interaction with W193 of the conserved WPD loop. The conformation of R233 side chain is further stabilized by a salt-bridge interaction with conserved E133 (Fig. 3A). This position of the R233 side chain allows room for the disulfide bond formation between the catalytic C227 and C129 (Fig. 2C, 3A), a residue highly conserved only in PEST-enriched phosphatases (Fig. 2B). As a result, the catC227 $S\gamma$ is not facing the phosphate ion in our structure.

Phosphate at the catalytic site

From the early stages of structural refinement, a well-ordered, tetrahedral-shaped density was observed near the P-loop and catC227 (Fig. 2A, 2C). Although both ammonium sulfate and potassium phosphate were present in the crystallization mother liquor, the tetrahedral densities were assigned as phosphate ions, in accordance with the phosphatase activity of the protein. The phosphate ion is well defined with strong electron density and low B-factors (Fig. 2C). The oxygen atoms of the phosphate ion interact with the backbone amide nitrogen atoms of the residues belonging to P-loop (Fig. 3A) and its position matches well with that of the tungstate ion, coordinated by the PTP-1B P-loop (PDB code: 2HNQ) (Fig. 3B). However, no hydrogen bond between the phosphate ion and the guanidinium nitrogen atoms of the signature motif arginine (R233) is observed in LYPcat, although it is weakly present in tungstate bound PTP-1B. The series of structures of Cdc25B solved by Buhrman et al. (12) revealed a disulfide bond of the catalytic Cys with a back-door Cys (PDB code: 1YS0). However in this structure, the P-loop of Cdc25B has folded over the catalytic Cys like a lid, preventing access of the substrate to the catalytic pocket. When this structure is compared to the sulfate-bound Cdc25B structure (PDB entry 1QB0), they find that the main chain of the P-loop of the disulfide formed structure occupies the same location as the sulfate ion. It is suggested that this conformational change in the P-loop of Cdc25B disulfide structure is to allow room for the disulfide bond to

form, since steric restraints prevent the movement of the WPD loop and the active-site arginine (35). In comparison, the P-loop of LYPcat is much more similar to the sulfate-bound structure of Cdc25B (36), with the catalytic pocket accessible to substrate. Thus, the WPD loop and active site arginine in LYPcat are presumably able to move in response to disulfide bond formation, and do not require the movement of the P-loop to compensate. Buhrman *et al.* note that the catalytic Cys in their structure is not able to bind substrate without significant conformational rearrangement by breaking the disulfide bond.

Novel mechanism of redox regulation of LYP activity

The presence of an extra Cys in the P-loop, and the participation of the back-door Cys in the disulfide bond as revealed in this structure, suggest a potential function for protecting the essential catalytic Cys from oxidative damage, while also regulating the activity of LYPcat. The catalytic Cys of PTPs is known to be highly reactive to phosphotyrosines and highly susceptible to H₂O₂ oxidation (26) due to its microenvironment and its low pKa (4.7-5.4) (37). Oxidation of the essential Cys prevents enzymatic dephosphorylation because catalysis involves a covalently bound phospho-Cys intermediate that cannot form if the Cys has been oxidized. Under relatively mild oxidation conditions, this oxidation to sulfenic acid (Cys-SOH) is reversible through reduction by thiols. Highly oxidizing conditions lead to the irreversibly oxidized sulfinic acid (Cys-SO₂) and sulfonic acid (Cys-SO₃) states, which completely inactivate PTPs. Thus far, PTPs have shown three different methods of protection from H₂O₂ oxidation—classical PTPs form sulfenylamide rings with the neighboring amide from the main chain of the serine in the P-loop (21,30,31,38), Cdc25, VHR, and PTEN form disulfides with a back-door Cys outside of the P-loop (12,13,27-29,39,40), and the low molecular weight PTP forms a disulfide with a Cys found within the P-loop (23,41). Interestingly, LYPcat is a classical PTP, but our structure does not contain the expected cyclic sulfenamide. Rather, catC227 is found in a disulfide bond with a back-door Cys, C129, a state previously only found in non-classical PTPs. Another notable feature found in our protein shows that there is also another Cys found in the P-loop, potentially allowing for a secondary site to form a disulfide bond. To date, classical PTPs have not been shown to have a mode of redox regulation aside from the cyclic sulfenamide.

To get a better understanding of what might be happening during redox regulation of LYP, we created 3 mutants on C129 and C231, the two potential disulfide partners of the catC227 – single point mutants C129S, C231S, and a double mutant C129S-C231S. One of the initial concerns was whether the mutants still retained activity. We found that C129S has 48% of wild type activity, while C231S and C129S-C231S both have 13% of wild type activity (Fig. 4A, 4C). The significantly reduced specific activity of C231S suggests its importance for catalysis. The double mutant, C129S-C231S has similar specific activity to C231S, indicating that the additional C129S mutation does not significantly reduce the activity of the protein further. Thus, the effect of each separate mutation is not additive.

We then sought to understand the roles of each of the Cys in redox regulation of LYPcat. In T cells, rapid production of ROS is known to accompany TCR signaling (41-43). Recently the tyrosine phosphatase SHP-2 has been reported to be regulated by ROS during TCR signaling (44). ROS may affect TCR signaling through regulation of the activity of LYP as well. In accordance, we added 100 μM H₂O₂ and incubated for 10 minutes to the wild type and its mutants, finding that peroxide completely inactivated all of the proteins (Fig. 4C). Oxidation of PTPs is known to sequester the catalytic Cys such that it cannot functionally work as a phosphatase. Across the PTP superfamily, it has been shown that various methods of protection for the catalytic Cys from highly oxidizing conditions allow for some reversibility under reducing conditions that can recover the active thiolate form of the catalytic Cys. To test whether this property is conserved in wild type LYPcat and its mutants (Fig. 4B and 4C), we

attempted recovery of activity by incubating with 10mM DTT for 15 minutes. The results showed that wild type recovers to about 25% of its original activity. Lack of 100% recovery was somewhat expected since reactivation kinetics by thiols is estimated to be 10-100 times slower than inactivation by H₂O₂ (39). Reactivation studies by Denu and Tanner (39) show that after 15 minutes, VHR and PTP1 (rat) are only at about 20-25% of the maximal activation shown in their studies. In addition, since H₂O₂ is a strong oxidizer, some active centers may have been irreversibly oxidized, preventing 100% recovery. Interestingly, in the time over which the mutants were studied, percent reactivation in the C231S (63%) and C129S-C231S double mutant (43%) appeared to be significantly higher than wild type (25%). However, the other single mutant, C129S, had a lower percent reactivation (18%) than wild type. The rate of catalysis of the reactivated samples remained constant over the time period measured (data not shown). Further, since the reactivation by DTT is continuous, even during measurement, we can conclude that reactivation is complete.

The reduction in reactivation of the C129S mutant after H₂O₂ treatment suggests that this residue is important in protecting catC227 from irreversible oxidation. Together with the structural data, these results suggest that at least one method of protection of LYP from ROS inactivation is through the disulfide bond between catC227 and the back-door C129. The C231S mutant, which shows a greater percent reactivation than wildtype, still has the C129 available for disulfide bond formation and the difference in reactivation between the C231S and C129S-C231S mutants can be similarly attributed to C129 availability for oxidation protection. Distances between the α carbon atoms of C129 and C227 in publicly available LYPcat structures (PDB codes: 2P6X, 2QCT, 2QCJ) is 4.9-5.4Å, and the distance in the disulfide bonded structure is 5.6Å, all of which are in the normal range (4.4-6.8Å) of C α -C α distance of disulfide bonds (26). Thus, the disulfide bond between C129 and catC227 can be formed without any significant conformational change in the structure, involving just a rotation around χ_1 for catC227.

While the role of C129 seems clear given previous studies on the back-door Cys, the role of C231 and its interaction with catC227 and C129 are not as straightforward. Given the higher reactivation rate of both C231S mutants, it appears that C231 suppresses reactivation in a reducing environment. One possibility is that C231 may be competing with C227 for reduction in the catalytic pocket. In the C231S mutant, catC227 would be free to be reduced, thus allowing LYPcat to recover activity even greater than wildtype enzyme. Since gain-of-function of LYP has been linked to autoimmunity, it is possible that C231 evolved as a mechanism of negative regulation of LYP, which results in overall prevention of autoimmune diseases. Classical PTPs have previously demonstrated protection from oxidation through formation of a cyclic sulfenamide (22,30) between the catalytic Cys and the main chain amide from the neighboring serine in the classical PTP signature motif HCSXGXGR[T/S]G.

Concluding Remarks

LYP is a negative downstream regulator of T-cell signaling, and a drug target for autoimmunity. In this manuscript, we present a crystal structure of LYPcat involving an intramolecular disulfide bond with a phosphate bound in the catalytic pocket. We demonstrate that LYP, a classical PTP, forms this disulfide bond primarily with a back-door Cys, C129 in response to an oxidizing environment, a protective mechanism not previously seen in this class of PTPs. Surprisingly, C231 seems to play a role opposite to that of C129 in negatively regulating catalysis by inhibiting reactivation in a reducing environment. We propose that C129 and C231 comprise a yin-yang pair working as a built-in auto-regulation circuit for this enzyme playing a critical role in T cell activation and autoimmunity.

Acknowledgments

We thank Divya Krishnamurthy and Lauren Holden for enlightening experimental discussions, and Tiffanie Nham for technical assistance in purification of the mutant proteins.

References

- Hunter T. A thousand and one protein kinases. *Cell* 1987;50:823–829. [PubMed: 3113737]
- Mustelin T, Abraham RT, Rudd CE, Alonso A, Merlo JJ. Protein tyrosine phosphorylation in T cell signaling. *Frontiers in bioscience : a journal and virtual library* 2002;7:d918–969. [PubMed: 11897562]
- Mustelin T, Feng GS, Bottini N, Alonso A, Kholod N, Birle D, Merlo J, Huynh H. Protein tyrosine phosphatases. *Frontiers in bioscience : a journal and virtual library* 2002;7:d85–142. [PubMed: 11779706]
- Fischer EH, Charbonneau H, Tonks NK. Protein tyrosine phosphatases: a diverse family of intracellular and transmembrane enzymes. *Science (New York, NY)* 1991;253:401–406.
- Mustelin T, Taskén K. Positive and negative regulation of T-cell activation through kinases and phosphatases. *The Biochemical journal* 2003;371:15–27. [PubMed: 12485116]
- Tonks NK, Neel BG. From form to function: signaling by protein tyrosine phosphatases. *Cell* 1996;87:365–368. [PubMed: 8898190]
- Walton KM, Dixon JE. Protein tyrosine phosphatases. *Annual Review of Biochemistry* 1993;62:101–120.
- Alonso A, Sasin J, Bottini N, Friedberg I, Osterman A, Godzik A, Hunter T, Dixon J, Mustelin T. Protein tyrosine phosphatases in the human genome. *Cell* 2004;117:699–711. [PubMed: 15186772]
- Andersen JN, Mortensen OH, Peters GH, Drake PG, Iversen LF, Olsen OH, Jansen PG, Andersen HS, Tonks NK, Møller NP. Structural and evolutionary relationships among protein tyrosine phosphatase domains. *Molecular and cellular biology* 2001;21:7117–7136. [PubMed: 11585896]
- Bottini N, Bottini E, Gloria-Bottini F, Mustelin T. Low-molecular-weight protein tyrosine phosphatase and human disease: in search of biochemical mechanisms. *Archivum immunologiae et therapiae experimentalis* 2002;50:95–104. [PubMed: 12022706]
- Bottini N, Musumeci L, Alonso A, Rahmouni S, Nika K, Rostamkhani M, MacMurray J, Meloni GF, Lucarelli P, Pellecchia M, Eisenbarth GS, Comings D, Mustelin T. A functional variant of lymphoid tyrosine phosphatase is associated with type I diabetes. *Nature genetics* 2004;36:337–338. [PubMed: 15004560]
- Buhrman G, Parker B, Sohn J, Rudolph J, Mattos C. Structural mechanism of oxidative regulation of the phosphatase Cdc25B via an intramolecular disulfide bond. *Biochemistry* 2005;44:5307–5316. [PubMed: 15807524]
- Kozlov G, Cheng J, Ziomek E, Banville D, Gehring K, Ekiel I. Structural insights into molecular function of the metastasis-associated phosphatase PRL-3. *The Journal of biological chemistry* 2004;279:11882–11889. [PubMed: 14704153]
- Tonks NK, Neel BG. Combinatorial control of the specificity of protein tyrosine phosphatases. *Current opinion in cell biology* 2001;13:182–195. [PubMed: 11248552]
- Wang Z, Shen D, Parsons DW, Bardelli A, Sager J, Szabo S, Ptak J, Silliman N, Peters BA, van der Heijden MS, Parmigiani G, Yan H, Wang TL, Riggins G, Powell SM, Willson JK, Markowitz S, Kinzler KW, Vogelstein B, Velculescu VE. Mutational analysis of the tyrosine phosphatome in colorectal cancers. *Science (New York, NY)* 2004;304:1164–1166.
- Wu H, Cantor RM, Graham DS, Lingren CM, Farwell L, Jager PL, Bottini N, Grossman JM, Wallace DJ, Hahn BH, Julkunen H, Hebert LA, Rovin BH, Birmingham DJ, Rioux JD, Yu CY, Kere J, Vyse TJ, Tsao BP. Association analysis of the R620W polymorphism of protein tyrosine phosphatase PTPN22 in systemic lupus erythematosus families: increased T allele frequency in systemic lupus erythematosus patients with autoimmune thyroid disease. *Arthritis and rheumatism* 2005;52:2396–2402. [PubMed: 16052563]

17. Cloutier JF, Veillette A. Cooperative inhibition of T-cell antigen receptor signaling by a complex between a kinase and a phosphatase. *The Journal of experimental medicine* 1999;189:111–121. [PubMed: 9874568]
18. Begovich AB, Carlton VE, Honigberg LA, Schrodi SJ, Chokkalingam AP, Alexander HC, Ardlie KG, Huang Q, Smith AM, Spoerke JM, Conn MT, Chang M, Chang SY, Saiki RK, Catanese JJ, Leong DU, Garcia VE, McAllister LB, Jeffery DA, Lee AT, Batliwalla F, Remmers E, Criswell LA, Seldin MF, Kastner DL, Amos CI, Sninsky JJ, Gregersen PK. A missense single-nucleotide polymorphism in a gene encoding a protein tyrosine phosphatase (PTPN22) is associated with rheumatoid arthritis. *American journal of human genetics* 2004;75:330–337. [PubMed: 15208781]
19. Kyogoku C, Langefeld CD, Ortmann WA, Lee A, Selby S, Carlton VE, Chang M, Ramos P, Baechler EC, Batliwalla FM, Novitzke J, Williams AH, Gillett C, Rodine P, Graham RR, Ardlie KG, Gaffney PM, Moser KL, Petri M, Begovich AB, Gregersen PK, Behrens TW. Genetic association of the R620W polymorphism of protein tyrosine phosphatase PTPN22 with human SLE. *American journal of human genetics* 2004;75:504–507. [PubMed: 15273934]
20. Vang T, Congia M, Macis MD, Musumeci L, Orrú V, Zavattari P, Nika K, Tautz L, Taskén K, Cucca F, Mustelin T, Bottini N. Autoimmune-associated lymphoid tyrosine phosphatase is a gain-of-function variant. *Nature genetics* 2005;37:1317–1319. [PubMed: 16273109]
21. den Hertog J, Groen A, van der Wijk T. Redox regulation of protein-tyrosine phosphatases. *Archives of biochemistry and biophysics* 2005;434:11–15. [PubMed: 15629103]
22. Groen A, Lemeer S, van der Wijk T, Overvoorde J, Heck AJ, Ostman A, Barford D, Slijper M, den Hertog J. Differential oxidation of protein-tyrosine phosphatases. *J Biol Chem* 2005;280:10298–10304. [PubMed: 15623519]
23. Caselli A, Marzocchini R, Camici G, Manao G, Moneti G, Pieraccini G, Ramponi G. The inactivation mechanism of low molecular weight phosphotyrosine-protein phosphatase by H₂O₂. *The Journal of biological chemistry* 1998;273:32554–32560. [PubMed: 9829991]
24. Xing K, Raza A, Löfgren S, Fernando MR, Ho YS, Lou MF. Low molecular weight protein tyrosine phosphatase (LMW-PTP) and its possible physiological functions of redox signaling in the eye lens. *Biochimica et biophysica acta* 2007;1774:545–555. [PubMed: 17428749]
25. Chiarugi P, Fiaschi T, Taddei ML, Talini D, Giannoni E, Raugei G, Ramponi G. Two vicinal cysteines confer a peculiar redox regulation to low molecular weight protein tyrosine phosphatase in response to platelet-derived growth factor receptor stimulation. *The Journal of biological chemistry* 2001;276:33478–33487. [PubMed: 11429404]
26. Cho SH, Lee CH, Ahn Y, Kim H, Ahn CY, Yang KS, Lee SR. Redox regulation of PTEN and protein tyrosine phosphatases in H₂O₂ mediated cell signaling. *FEBS Lett* 2004;560:7–13. [PubMed: 15017976]
27. Fauman EB, Cogswell JP, Lovejoy B, Rocque WJ, Holmes W, Montana VG, Piwnicka-Worms H, Rink MJ, Saper MA. Crystal structure of the catalytic domain of the human cell cycle control phosphatase, Cdc25A. *Cell* 1998;93:617–625. [PubMed: 9604936]
28. Lee SR, Yang KS, Kwon J, Lee C, Jeong W, Rhee SG. Reversible inactivation of the tumor suppressor PTEN by H₂O₂. *The Journal of biological chemistry* 2002;277:20336–20342. [PubMed: 11916965]
29. Sohn J, Rudolph J. Catalytic and chemical competence of regulation of cdc25 phosphatase by oxidation/reduction. *Biochemistry* 2003;42:10060–10070. [PubMed: 12939134]
30. Salmeen A, Andersen JN, Myers MP, Meng TC, Hinks JA, Tonks NK, Barford D. Redox regulation of protein tyrosine phosphatase 1B involves a sulphenyl-amide intermediate. *Nature* 2003;423:769–773. [PubMed: 12802338]
31. van Montfort RL, Congreve M, Tisi D, Carr R, Jhoti H. Oxidation state of the active-site cysteine in protein tyrosine phosphatase 1B. *Nature* 2003;423:773–777. [PubMed: 12802339]
32. The CCP4 suite: programs for protein crystallography. *Acta Crystallogr D Biol Crystallogr* 1994;50:760–763. [PubMed: 15299374]
33. Yu X, Sun JP, He Y, Guo X, Liu S, Zhou B, Hudmon A, Zhang ZY. Structure, inhibitor, and regulatory mechanism of Lyp, a lymphoid-specific tyrosine phosphatase implicated in autoimmune diseases. *Proceedings of the National Academy of Sciences of the United States of America* 2007;104:19767–19772. [PubMed: 18056643]

34. Barr AJ, Ugochukwu E, Lee WH, King ON, Filippakopoulos P, Alfano I, Savitsky P, Burgess-Brown NA, Muller S, Knapp S. Large-scale structural analysis of the classical human protein tyrosine phosphatome. *Cell* 2009;136:352–363. [PubMed: 19167335]
35. Gruninger RJ, Brent Selinger L, Mosimann SC. Effect of ionic strength and oxidation on the P-loop conformation of the protein tyrosine phosphatase-like phytase, PhyAsr. *The FEBS journal* 2008;275:3783–3792. [PubMed: 18573100]
36. Reynolds RA, Yem AW, Wolfe CL, Deibel MR, Chidester CG, Watenpaugh KD. Crystal structure of the catalytic subunit of Cdc25B required for G2/M phase transition of the cell cycle. *Journal of molecular biology* 1999;293:559–568. [PubMed: 10543950]
37. Denu JM, Dixon JE. Protein tyrosine phosphatases: mechanisms of catalysis and regulation. *Curr Opin Chem Biol* 1998;2:633–641. [PubMed: 9818190]
38. Yang J, Groen A, Lemeer S, Jans A, Slijper M, Roe SM, den Hertog J, Barford D. Reversible oxidation of the membrane distal domain of receptor PTPalpha is mediated by a cyclic sulfenamide. *Biochemistry* 2007;46:709–719. [PubMed: 17223692]
39. Denu JM, Tanner KG. Specific and reversible inactivation of protein tyrosine phosphatases by hydrogen peroxide: evidence for a sulfenic acid intermediate and implications for redox regulation. *Biochemistry* 1998;37:5633–5642. [PubMed: 9548949]
40. Sun JP, Wang WQ, Yang H, Liu S, Liang F, Fedorov AA, Almo SC, Zhang ZY. Structure and biochemical properties of PRL-1, a phosphatase implicated in cell growth, differentiation, and tumor invasion. *Biochemistry* 2005;44:12009–12021. [PubMed: 16142898]
41. Salmeen A, Barford D. Functions and mechanisms of redox regulation of cysteine-based phosphatases. *Antioxidants & redox signaling* 2005;7:560–577. [PubMed: 15890001]
42. Meng TC, Buckley DA, Galic S, Tiganis T, Tonks NK. Regulation of insulin signaling through reversible oxidation of the protein-tyrosine phosphatases TC45 and PTP1B. *J Biol Chem* 2004;279:37716–37725. [PubMed: 15192089]
43. Yamamura H. Redox control of protein tyrosine phosphorylation. *Antioxid Redox Signal* 2002;4:479–480. [PubMed: 12215215]
44. Kwon J, Qu CK, Maeng JS, Falahati R, Lee C, Williams MS. Receptor-stimulated oxidation of SHP-2 promotes T-cell adhesion through SLP-76-ADAP. *EMBO J* 2005;24:2331–2341. [PubMed: 15933714]

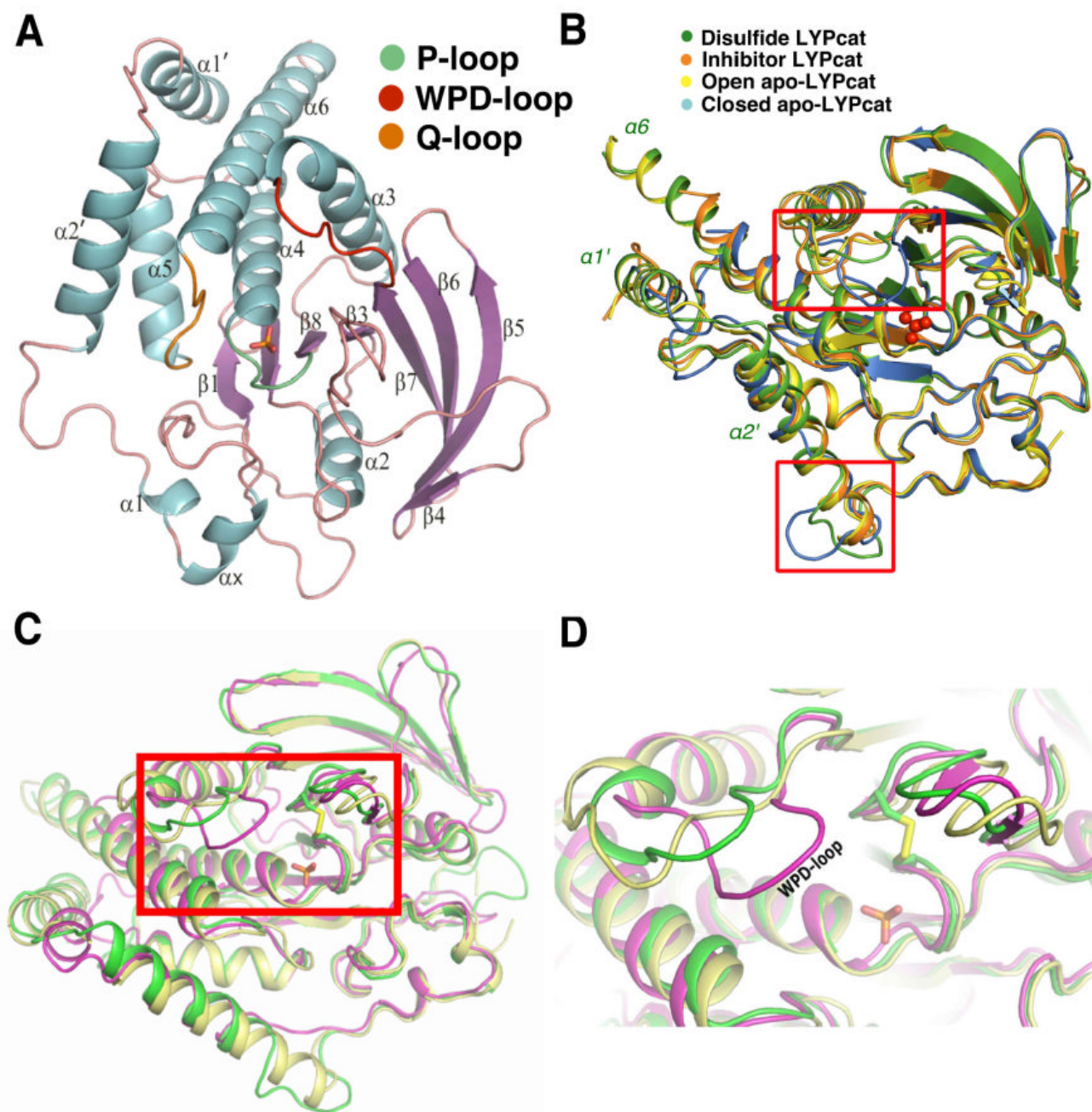


Fig. 1. LYP Structure and comparison to other PTPs. A. Ribbon diagram of LYP catalytic domain (LTPcat). Alpha helices are in blue, beta sheets are colored purple, the P-loop is colored green, the WPD loop is red, the Q-loop is orange, and all other loops are pink. The bound phosphate ion at the active site is shown as a stick model. B. The superposition of known structures of LYPcat, with the major areas of differences in surface loops indicated by the red boxes. The structure in this report is shown in green, LYPcat with an inhibitor (PDB code: 2QCT) in orange, corresponding structure without inhibitor (PDB code: 2QCJ) in blue, and the LYPcat alone with the PDB code 2P6X in yellow. The phosphate ion is shown in red ball and stick. C. Comparison of the different WPD loop conformations between LYPcat (shown in green), non-

phosphate-bound LYPCat (in yellow, PDB code: 2P6X) and the tungstate bound PTP1B (in magenta, PDB code: 2HNQ). Phosphate ion and disulfide bond of LYPCat are shown as sticks. D. Zoomed view of the boxed area in Fig 1C, showing different locations of WPD loop in the three structures.

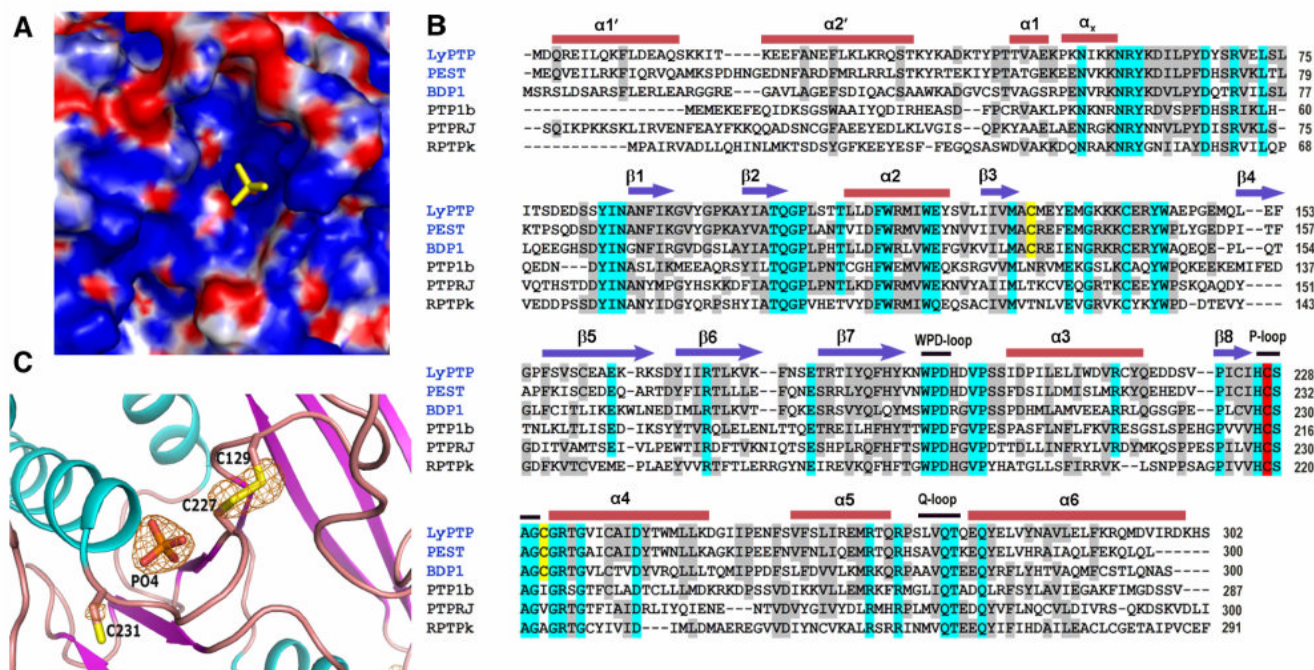


Fig. 2.

Binding of the phosphate ion in active site of LYPCat and sequence alignment: A. Surface electrostatic potential of phosphate bound LYPCat, phosphate ion (in yellow) is located in a deep cleft of the surface. B. Sequence and secondary structure alignment of LYPCat with other members of the NT4 subfamily and PTP-1B, PTPRJ and RTPPk. Arrows represent β -strands, bars denote α -helices, and black lines denote catalytically important loops. The catalytic cysteine is highlighted in red and the two other cysteines around the catalytic site are highlighted in yellow. Residues conserved in all the sequences are highlighted in cyan and those showing at least 50% conservation in grey. The names of the NT4 subfamily are given in blue. C. $F_o - F_c$ map is shown around the phosphate ion and disulfide bridge at a contour level of 4.5σ . Map was calculated where these atoms were omitted from the final coordinates. Alpha helices are denoted in cyan, beta sheets are seen in purple, and loops are colored pink.

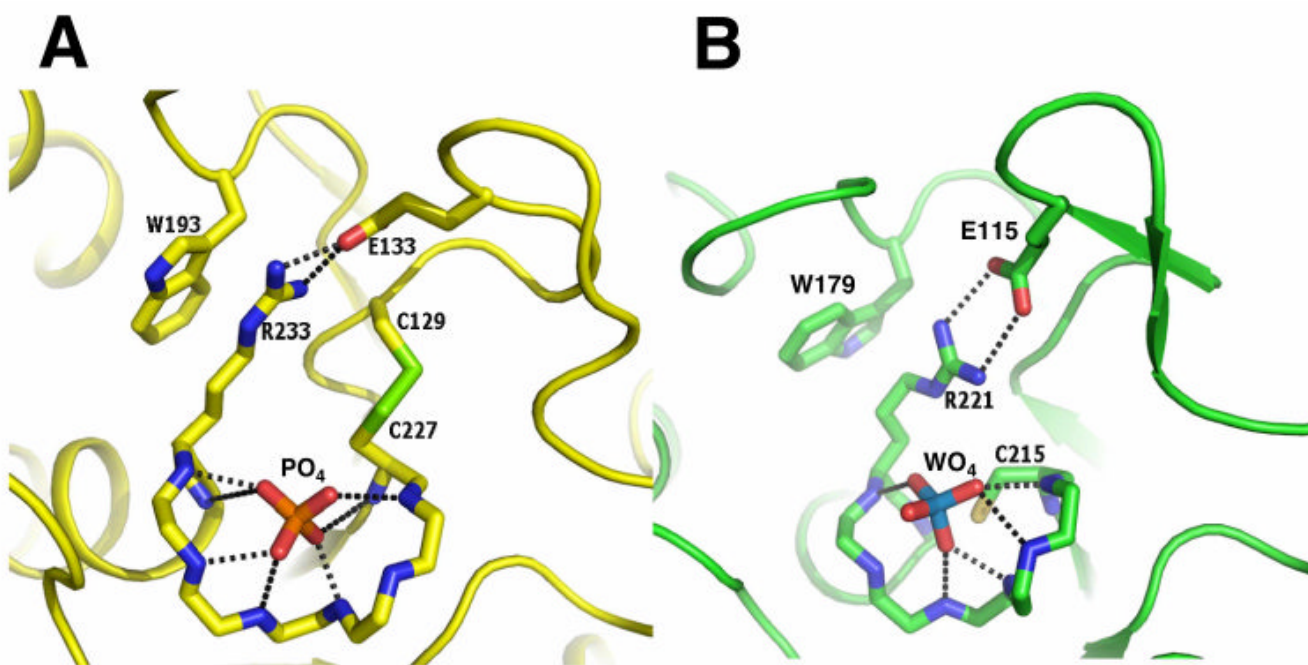


Fig. 3. Active site geometries of PTPs. A. Hydrogen bonds made by the active site phosphate ion in LYPcat with the amide nitrogen of the P-loop residues C227, S228, G230, C231, G232 and T234 and the interactions of R233 with W193 and E133. Side-chains of residues 228-232 were omitted for clarity. B. Interactions made by the active site tungstate ion with PTP-1B (coordinates taken from the PDB code 2HNQ), residues corresponding to R233, W193 and E233 are shown for comparison.

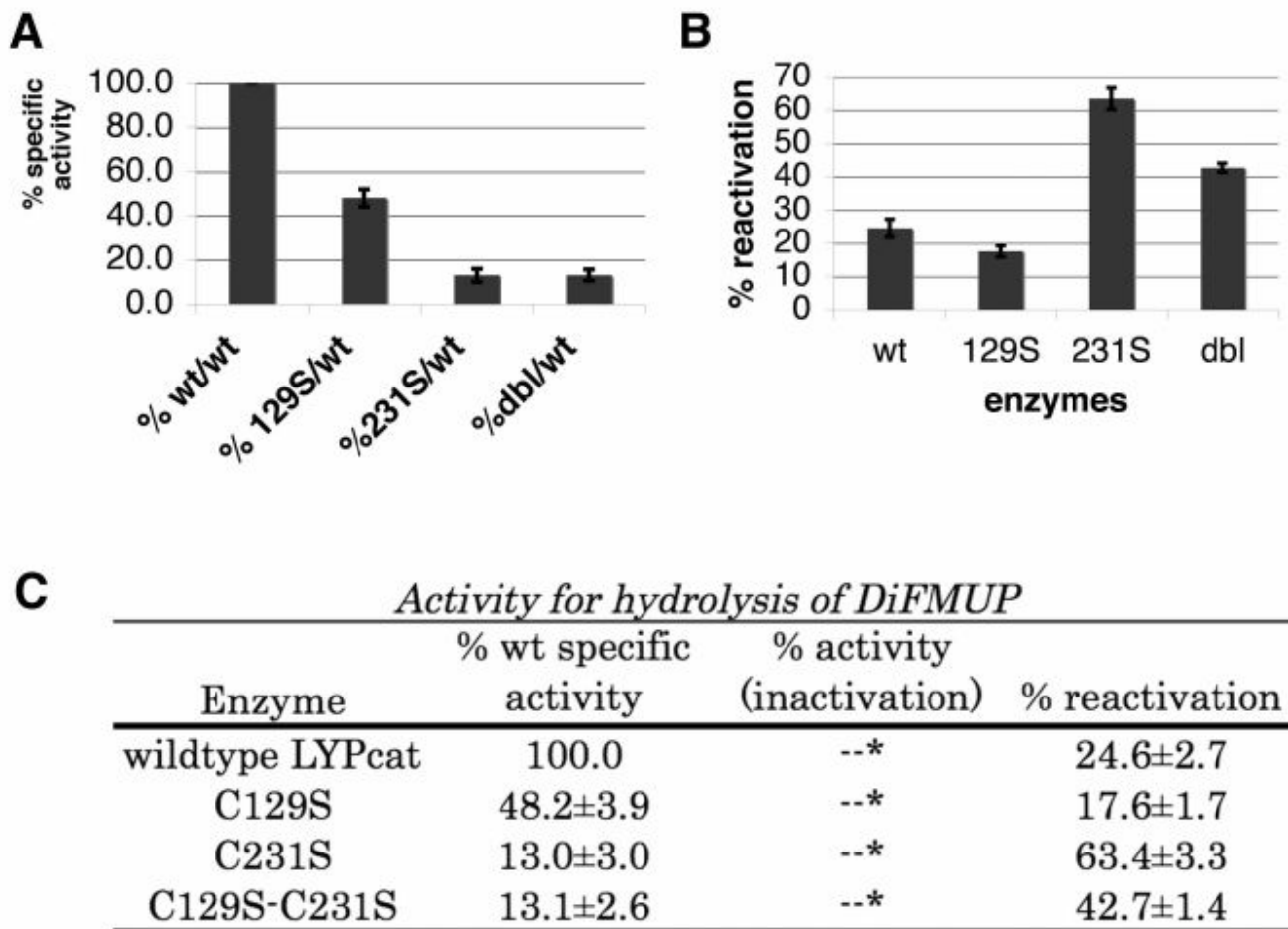


Fig. 4.

Phosphatase Activity Assays of LYP Mutants. A. Relative specific activity of each mutant protein compared to wild type using DiFMUP as the substrate. B. Percent activity of the reactivated proteins (H_2O_2 treated, followed by DTT treatment) relative to its own protein's full activity before H_2O_2 inactivation. DiFMUP was used as the substrate. All reactivation percentages of the mutants were found to be statistically significantly different from that of the wild type using the paired t-test. C. Summary of the activity assay results using DiFMUP as the substrate. Column 1 lists each protein, column 2 gives the specific activity of each protein, column 3 gives the percent activity of each protein after inactivation by H_2O_2 , column 4 gives the reactivation activity as a percentage of each protein's original activity after 10 minutes of inactivation by H_2O_2 , followed by DTT reactivation for 15 minutes.

Table 1

Crystallographic Statistics

Crystal Cell Parameters	
Space group	$P2_1$
Cell Dimensions	
(a, b, c in Å)	42.5, 68.9, 58.7
(β in °)	101.6
Data Collection Statistics	
Resolution Range (Å)	50.0-2.2
Observations	71791
Unique Reflections	16800
Completeness%	99.2 (92.2)
R_{sym} % (Last bin)	6.5 (26.9)
I/σ (Last bin)	19.1 (5.5)
Refinement Statistics	
R_{cryst} (%)	17.6
R_{free} (%)	20.4
RMS deviation	
Bond length (Å)	0.006
Bond angle (°)	1.6
Average B Factor (Å ²)	27.9

Note: $R_{\text{sym}} = \sum_{ij} |I_i(j) - \langle I(j) \rangle| / \sum_{ij} I_i(j)$, where $I_i(j)$ is the i -th measurement of reflection j and $\langle I(j) \rangle$ is the overall weighted mean of i measurements.
 $R_{\text{cryst}} = \sum_{hkl} ||F_o| - |F_c|| / \sum_{hkl} |F_o|$, 7% of the reflections were excluded for the R_{free} calculation.